



Northwest and
Alaska
Fisheries Center

National Marine
Fisheries Service

U.S. DEPARTMENT OF COMMERCE

NWAFRC PROCESSED REPORT 83-08

The Role of Migrations in Ecosystem Simulation

June 1983

NOTICE

This document is being made available in .PDF format for the convenience of users; however, the accuracy and correctness of the document can only be certified as was presented in the original hard copy format.

Inaccuracies in the OCR scanning process may influence text searches of the .PDF file. Light or faded ink in the original document may also affect the quality of the scanned document.

THE ROLE OF MIGRATIONS IN ECOSYSTEM SIMULATION

By

Nancy Pola Swan

Resource Ecology and Fisheries Management Division
Northwest and Alaska Fisheries Center
National Marine Fisheries Service
National Oceanic and Atmospheric Administration
2725 Montlake Boulevard East
Seattle, Washington 98112

June 1983

CONTENTS

	<u>Page</u>
Abstract.....	1
1. Introduction.....	2
2. General formulations of migration simulations.....	4
3. Simulation of seasonal migrations.....	5
4. Simulation of temperature-induced migrations.....	17
5. Results and discussion of migration simulations.....	24
6. References.....	28

LIST OF FIGURES AND TABLES

Figure 1.--DYNUMES Bering Sea 24x24 grid.

Figure 2a.--Autumn velocity field (in km/day) for yellowfin and rock sole seasonal migrations.

Figure 2b.--Spring velocity field (in km/day) for yellowfin and rock sole seasonal migrations.

Figure 3a.--Autumn velocity field (in km/day) for pollock seasonal migrations.

Figure 3b.--Spring velocity field (in km/day) for pollock seasonal migrations.

Figure 4a.--Monthly biomass change (in tens of kg/km^2) of yellowfin and rock sole due to seasonal migrations during October.

Figure 4b.--Monthly biomass change (in tens of kg/km^2) of yellowfin and rock sole due to seasonal migrations during November.

Figure 4c.--Monthly biomass change (in tens of kg/km^2) of yellowfin and rock sole due to seasonal migrations during May.

Figure 4d.--Monthly biomass change (in tens of kg/km^2) of yellowfin and rock sole due to seasonal migrations during June.

Figure 5a.--Monthly biomass change (in tens of kg/km^2) of pollock due to seasonal migrations during October.

Figure 5b.--Monthly biomass change (in tens of kg/km^2) of pollock due to seasonal migrations during November.

Figure 5c.--Monthly biomass change (in tens of kg/km^2) of pollock due to seasonal migrations during April.

Figure 5d.--Monthly biomass change (in tens of kg/km^2) of pollock due to seasonal migrations during May.

Figure 6a.--Monthly biomass change (in tens of kg/km^2) of king crab due to seasonal migrations during October.

Figure 6b.--Monthly biomass change (in tens of kg/km^2) of king crab due to seasonal migrations during November.

Figure 6c.--Monthly biomass change (in tens of kg/km^2) of king crab due to seasonal migrations during May.

Figure 6d.--Monthly biomass change (in tens of kg/km^2) of king crab due to seasonal migrations during June.

Figure 7a.--Mean Bering Sea bottom temperature for May (from Ingraham 1983).

Figure 7b.--Mean Bering Sea bottom temperature for June (from Ingraham 1983).

Figure 8a.--Velocity field (in km/day) for temperature-induced migrations of yellowfin and rock sole during May.

Figure 8b.--Velocity field (in km/day) for temperature-induced migrations of yellowfin and rock sole during June.

Figure 9a.--Velocity field (in km/day) for temperature-induced migrations of king crab during May.

Figure 9b.--Velocity field (in km/day) for temperature-induced migrations of king crab during June.

Figure 10a.--Mean Bering Sea surface temperature for May (from Ingraham 1983).

Figure 10b.--Mean Bering Sea surface temperature for June (from Ingraham 1983).

Figure 11a.--Velocity field (in km/day) for temperature-induced migrations of pollock during May.

Figure 11b.--Velocity field (in km/day) for temperature-induced migrations of pollock during June.

Figure 12a.--Summer (September) biomass distribution (in tens of kg/km^2) for yellowfin and rock sole.

Figure 12b.--Winter (February) biomass distribution (in tens of kg/km^2) for yellowfin and rock sole.

Figure 13a.--Summer (September) biomass distribution (in tens of kg/km^2) for pollock.

Figure 13b.--Winter (February) biomass distribution (in tens of kg/km^2) for pollock.

Figure 14a.--Summer (September) biomass distribution (in tens of kg/km^2) for king crab.

Figure 14b.--Winter (February) biomass distribution (in tens of kg/km^2) for king crab.

Table 1.--Species groupings in the DYNUMES model.

ABSTRACT

The Dynamical Numerical Marine Ecosystem Simulation (DYNUMES) model is unique in its ability to simulate, in addition to growth, apex predation, inter-species predation and fishery, spatial and temporal biomass distribution fluctuations caused by fish migrations. Two types of fish migration simulations are discussed: seasonal migrations for spawning and foraging and migrations to regions of optimum environmental conditions (optimum temperature).

The general formulation of migration simulation is a three-step process. First, migration velocities are calculated for each migrating species. Secondly, the migrating fraction of the biomass is separated from the non-migrating fraction. Finally, gradients in migrating biomass are calculated and the migrated biomass is computed using a finite difference advection equation. Migrations are simulated over a short time period for stability; several migration calculations are performed during each monthly model time step. At the end of each model month, conservation of biomass is enforced and random diffusion is simulated.

The specifics of the calculations as they apply to both seasonal and temperature-induced migrations are presented and the results are discussed. Migration simulation enhances the realism of ecosystem simulation models. In addition, it provides a means of studying spatial and temporal changes in predation mortality caused by changes in predator-prey overlap, fluctuations in biomass distributions caused by anomalous environmental conditions, and other space and time dependent factors in the ecosystem.

1. INTRODUCTION

The Dynamical Numerical Marine Ecosystem Simulation (DYNUMES) model, originally designed and implemented by Dr. Taivo Laevastu at Northwest and Alaska Fisheries Center (NAFCA), Seattle, has been used extensively to study ecosystem interactions in the eastern Bering Sea (e.g., Laevastu and Favorite 1978, 1979; Laevastu, et al., 1976; Laevastu and Marasco 1982). The model calculations are performed over a 24x24 grid covering over one million square kilometers in the eastern Bering Sea (Fig. 1), during each monthly model time step. The major dynamical processes simulated by the model are growth, apex predation by birds and mammals, inter- and intra-species predation and competition for food, and fishing mortality, all calculated for each of up to 27 species groups (see Table 1). In addition, the model simulates the temporal and spatial variability resulting from fish migrations. Three types of migrations are identified in the model: seasonal migrations for spawning and foraging, migrations induced by unfavorable environmental conditions (specifically, temperature), and migrations caused by scarcity of food. This paper presents the methods used in the simulations of the first two types of migrations, both of which occur, in the mean, in predictable spatial and temporal patterns.

The simulation of migration enhances the realism of the environmental simulation in several ways. First, it allows the representation of realistic seasonal changes in biomass distribution; second, geographical areas may be identified as being either sources or sinks of biomass in different seasons; finally, since seasonal migrations cause changes in predator-prey overlap, spatial and temporal changes in predation mortality may be examined.

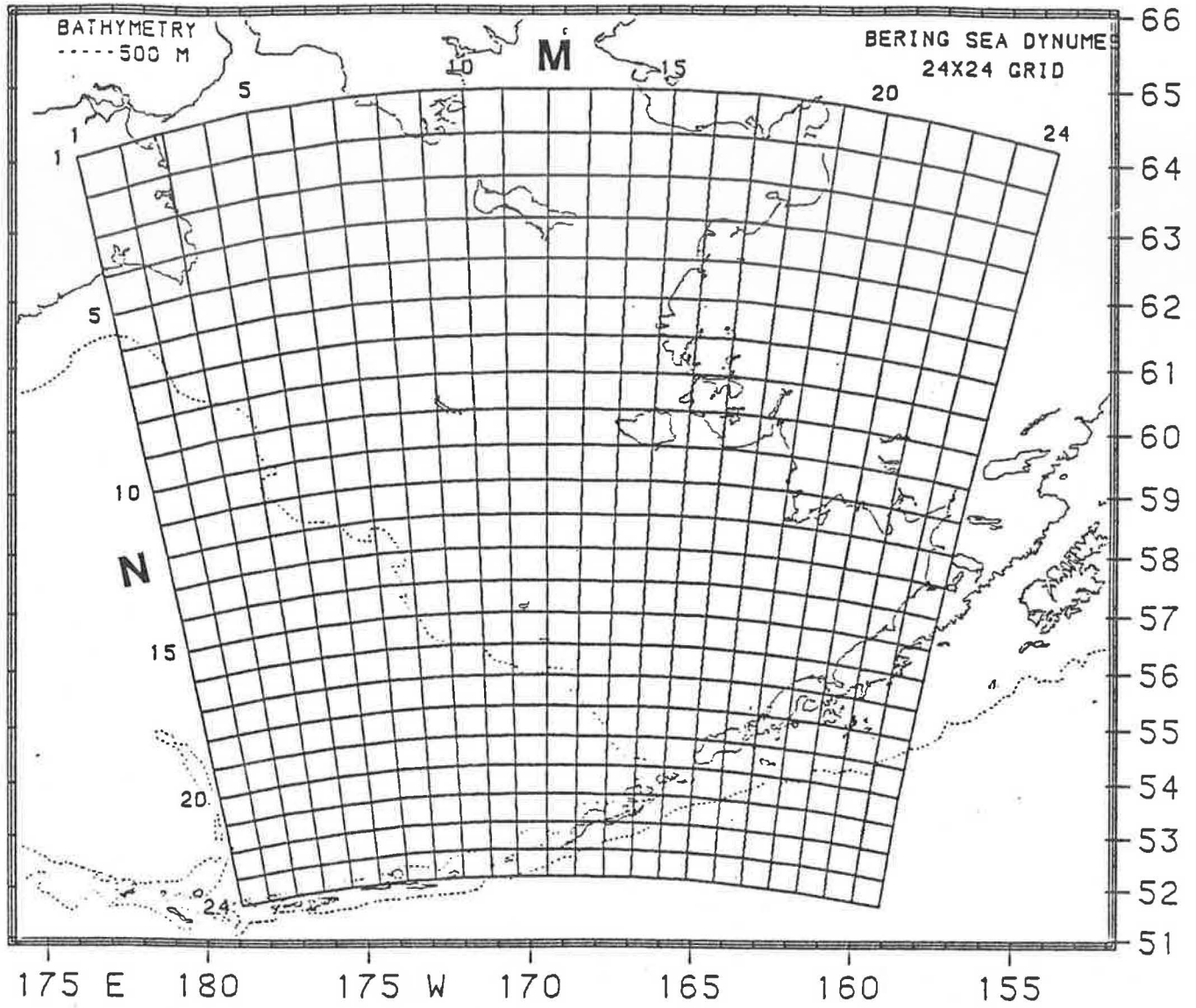


Figure 1.--DYNAMES Bering Sea 24x24 grid.

2. GENERAL FORMULATIONS OF MIGRATION SIMULATIONS

All migrations are calculated using the linear finite difference advection equation (Laevastu, 1976):

$$B_{t,n,m} = B_{t-1,n,m} - (t_d |U_{t,n,m}| UT_{n,m}) - (t_d |V_{t,n,m}| VT_{n,m}) \quad (1)$$

where B is the migrating biomass, t_d is the length of the migration time step, U and V are the east-west and north-south components, respectively, of the migration velocity, n is the row and m is the column of the grid point, and t is the model time step. UT and VT are gradients of the migrating biomass:

$$UT = (B_{n,m} - B_{n,m\pm 1})/L \quad (2)$$

$$VT = (B_{n,m} - B_{n\pm 1,m})/L \quad (3)$$

where L is the distance between adjacent grid points (63.5 km in the Bering Sea), and the biomass difference is taken in the upstream direction. Migrations are calculated using a two-day time step ($t_d=2$) for stability. The stability criterion is:

$$U t_d < L \quad (4)$$

where U is the maximum magnitude of either velocity component. Migration calculations are performed fifteen times during each monthly model time step. Conservation of biomass is enforced after each monthly model time step, since the advection equation is not fully conservative, using the formula:

$$B_{t+\Delta t,n,m} \leftarrow R * B_{t+\Delta t,n,m} \quad (5)$$

where

$$R = (\sum_{n,m} B_{t,n,m}) / (\sum_{n,m} B_{t+\Delta t,n,m}) \quad (6)$$

R is usually quite small.

3. SIMULATION OF SEASONAL MIGRATIONS

Seasonal fish migrations are caused by several factors, including migration to spawning grounds, searching for food, and searching for an optimum environment. In general, for most fish species in the eastern Bering Sea, there is an onshore migration during spring and an offshore migration during autumn. However, detailed components of the migration, such as the maximum depth of migration, latitudinal distribution of the migrating biomass, and locations of spawning grounds are species specific. Seasonal distribution and abundance of fish stocks are determined as accurately as possible from available survey data (Alverson 1960; Bakkala and Smith 1978; Smith 1979; Bakkala 1979; Pereyra et al. 1976; Niggol 1982). These temporal and spatial distributions are then simulated in the DYNUMES model and the results are again compared to available data. The model is initiated in August (month 8), since the Bering Sea data set is most complete for that month and input biomasses are best determined. Thereafter, the model can output the desired data fields at the end of each monthly time step for as many years as desired or as is possible under computer constraints.

The species groups used in the DYNUMES model are presented in Table 1. Spring migrations for most species are simulated during May and June. However, the model simulation of spring migrations for many pelagic species (e.g., Pacific Ocean perch, pollock) begins slightly earlier. Autumn migrations are generally simulated during October and November. Migrations are not simulated for cottids (species 11); there are insufficient data supporting long-range seasonal migrations in the Bering Sea for this species grouping. The abundance of salmon (species 17) in the Bering Sea varies seasonally as a function of the life stage; therefore, the abundance and distribution of salmon in the Bering Sea is prescribed seasonally in the DYNUMES model.

Table 1.--Species groupings in the DYNUMES model.

<u>Species Group No.</u>	<u>Species</u>
1-4	Used for special study
5	Halibut
6	Flathead sole, flounder
7	Yellowfin, rock sole
8	Other flatfish
9	Pacific Ocean perch
10	Sablefish
11	Cottids and other demersal species
12	Pollock
13	Pacific cod, saffron cod
14	Herring
15	Capelin and other pelagic species
16	Atka mackerel
17	Salmon
18	Squids
19	King crab
20	Tanner crab
21	Shrimp
22	Predatory benthos
23	Infauna
24	Epifauna
25	Copepods
26	Euphausiids
27	Phytoplankton

Seasonal migrations are simulated in DYNUMES by a three-step process. First, migration velocities in km/day are calculated for each species at each model grid point. In the second step the migrating fraction of the biomass is separated from the non-migrating fraction at each grid point. Finally, the biomass at each grid point is adjusted for changes due to migration, using equation (1), and conservation of biomass is enforced, using equation (5).

Seasonal migration velocities are calculated in the following manner. Using mean distribution patterns from summer and winter Bering Sea survey and commercial fishing data, an initial or "first guess" velocity is determined. The initial velocity is then modified by such species-specific variables as the minimum and maximum water depths of biomass distribution and longitudinal and latitudinal variations in distribution. In addition, velocities for known migrations into specific geographical areas, such as spawning grounds, may be simulated by addressing individual grid points. Two velocity fields are calculated for each species, one for spring and one for fall migrations; variations in migrations over several model years therefore reflect variations in the distribution of biomass before migration and not variations in the migration velocities, which are fixed. The spring and fall migration velocity vectors for yellowfin and rock sole (species group 7) and pollock (species 12) are shown in Figs. 2 and 3. The velocity fields for the two species are very similar; however, velocities for pollock have a stronger east-west component and those for yellowfin and rock sole are stronger in the north-south direction. The velocity fields for king crab (species 19; not shown) are virtually identical to those for yellowfin and rock sole.

After the seasonal migration velocities have been calculated, the migrating biomass is determined as a fraction of the biomass at each grid point. The migrating fraction is species specific and is estimated from available data. For

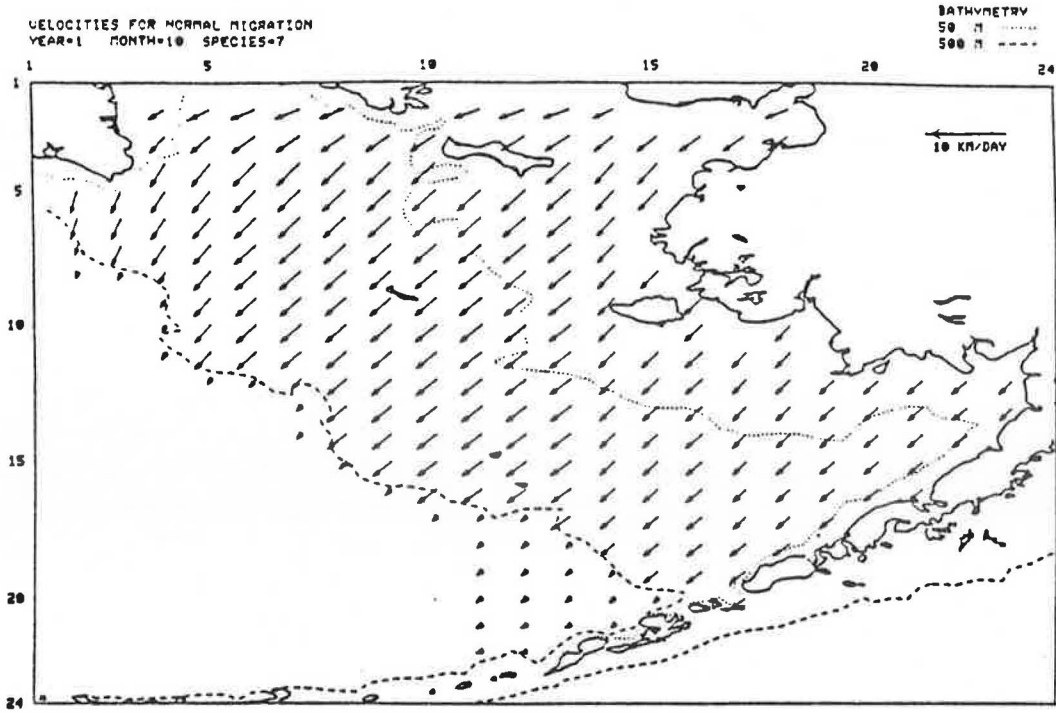


Figure 2a.--Autumn velocity field (in km/day) for yellowfin and rock sole seasonal migrations.

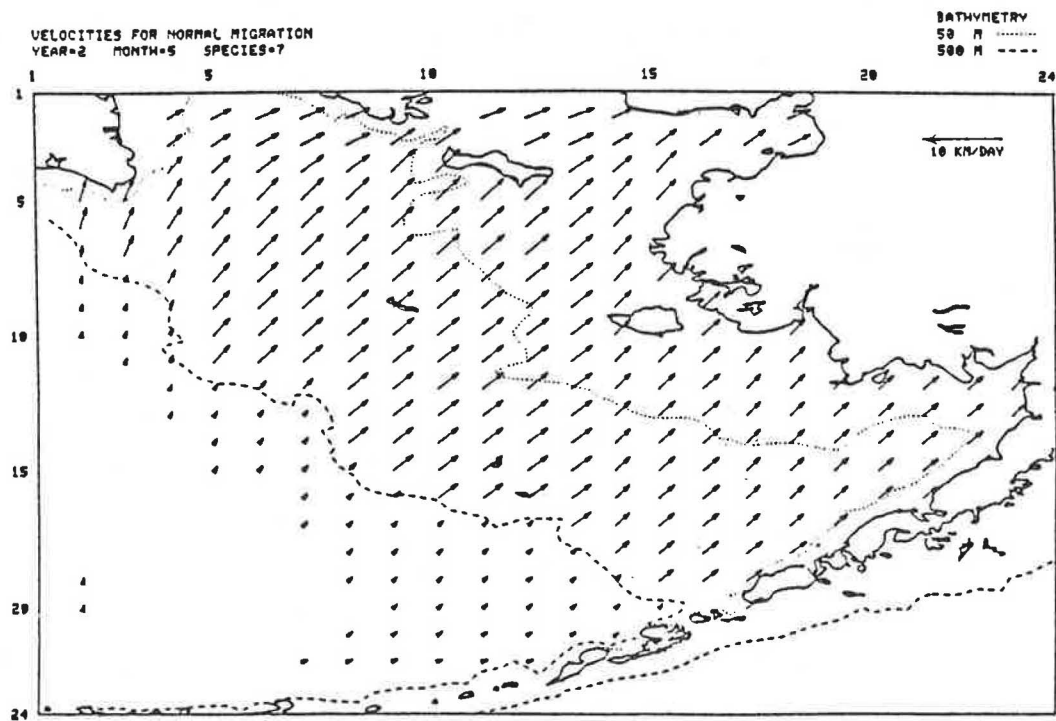


Figure 2b.--Spring velocity field (in km/day) for yellowfin and rock sole seasonal migrations.

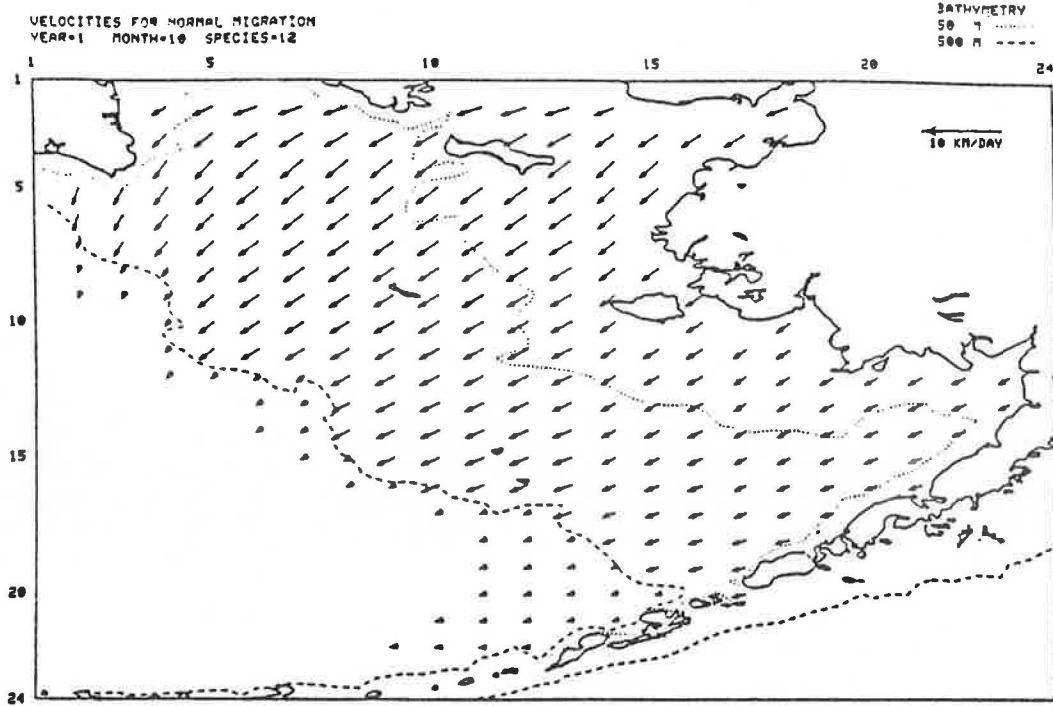


Figure 3a.--Autumn velocity field (in km/day) for pollock seasonal migrations.

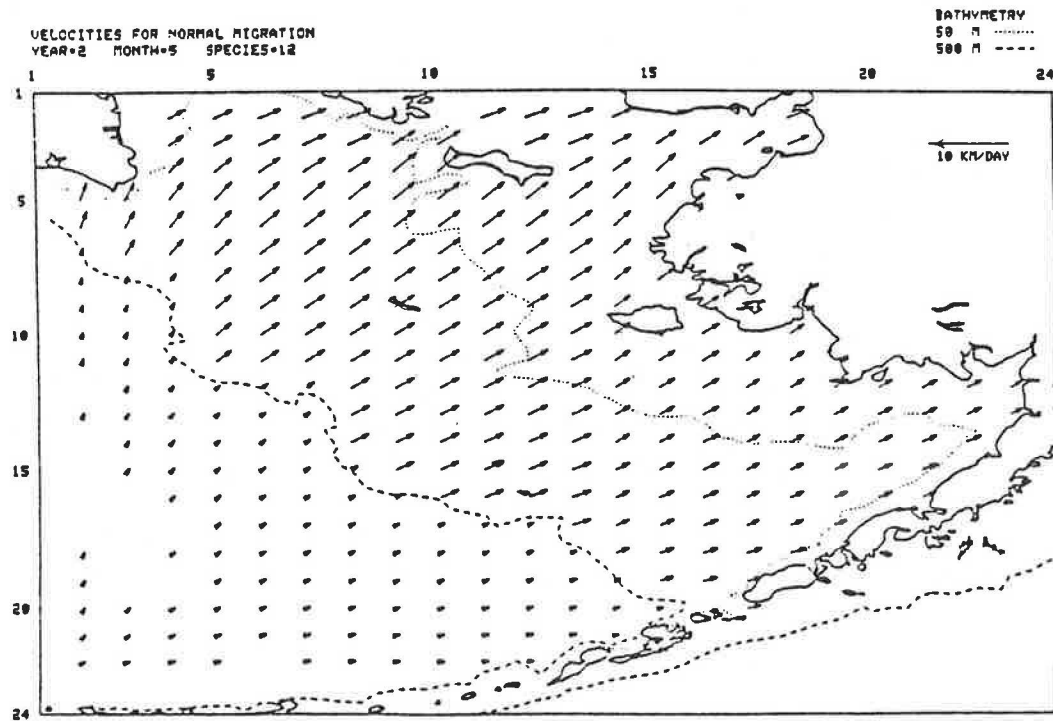


Figure 3b.--Spring velocity field (in km/day) for pollock seasonal migrations.

some species, such as herring, the spawning fraction of the biomass is used. For other species, the fraction is estimated from distribution and abundance data from fisheries survey cruises.

In the next step, the gradients of the migrating biomass in the direction of the migration velocity are calculated at each grid point using equations (2) and (3), assuming linearity between adjacent grid points. The migrated biomass is then calculated at each grid point using equation (1) for each two-day migration time step. This process is then repeated for a total of fifteen time steps, at which point conservation of biomass is enforced through equation (5). The resulting migration biomass is then smoothed over neighboring grid points to simulate random diffusion, using a nine-point Laplacian diffusion equation:

$$B_{n,m} = \alpha B_{n,m} + 1/4(1-\alpha) [B_{n-1,m} + B_{n+1,m} + B_{n,m-1} + B_{n,m+1}] \quad (7)$$

where α is a species-specific parameter designating the degree of smoothing desired. $\alpha=1$ for no smoothing and $\alpha=0$ for maximal smoothing. Typical values for α are between 0.7 and 0.95. Finally, the migrated biomass is added to the non-migrating biomass at each grid point.

Figures 4, 5, and 6 depict the monthly change in biomass due to seasonal migration for yellowfin and rock sole, pollock, and king crab, respectively, for autumn (year 1) and spring (year 2). The general offshore migration in autumn and onshore migration in spring can be seen. However, it is interesting to note that for all three species, the gradients in migration biomass are such that areas of convergence can be seen during the first autumn migration month, even though the velocity fields for autumn are uniformly offshore (see Figs. 2 and 3).

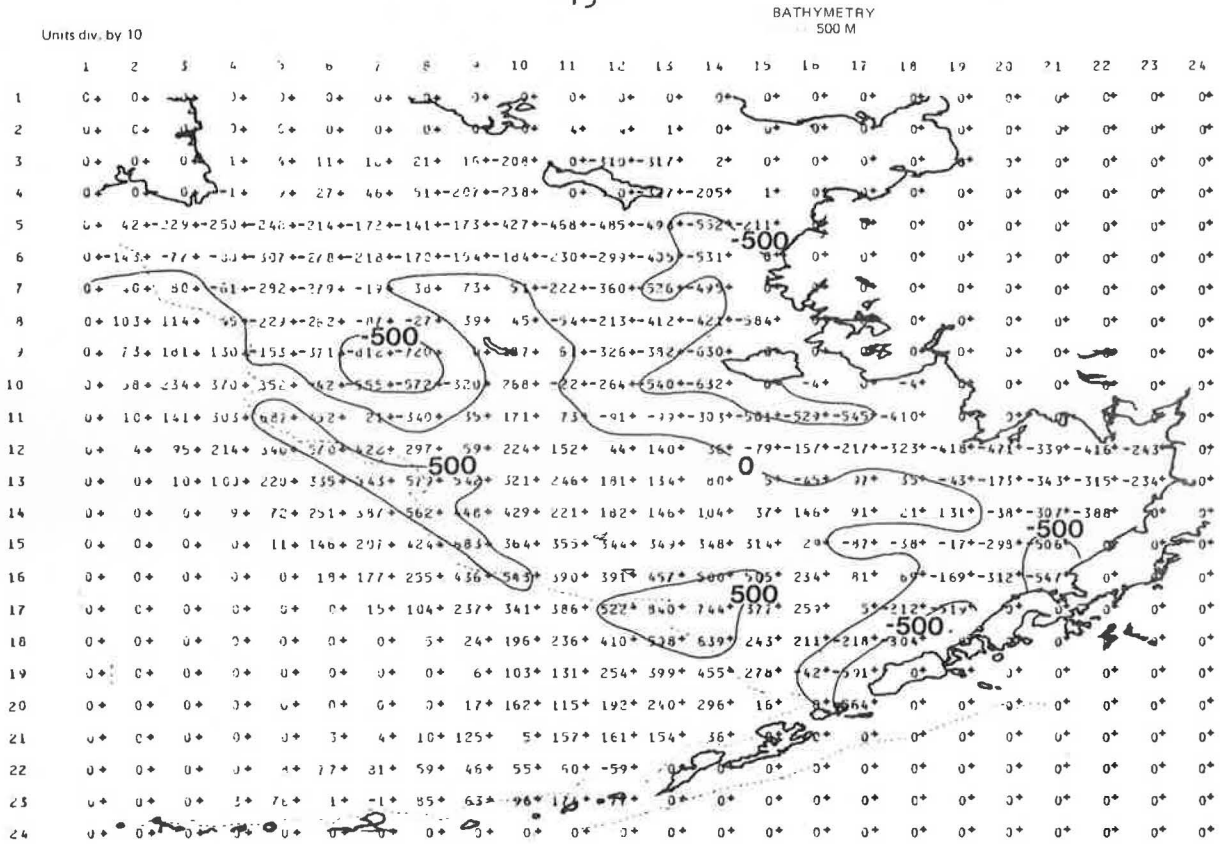


Figure 5a.--Monthly biomass change (in tens of kg/km²) of pollock due to seasonal migrations during October.

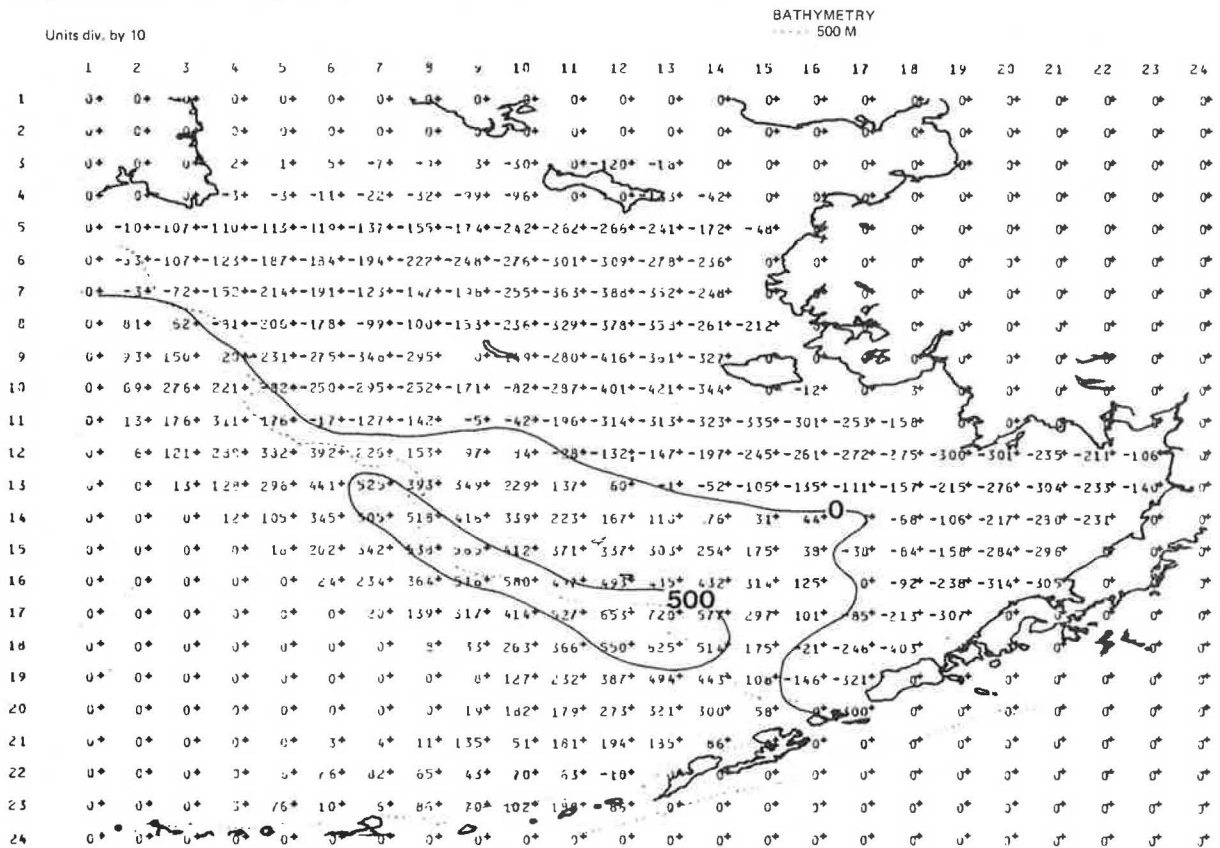


Figure 5b.--Monthly biomass change (in tens of kg/km²) of pollock due to seasonal migrations during November.

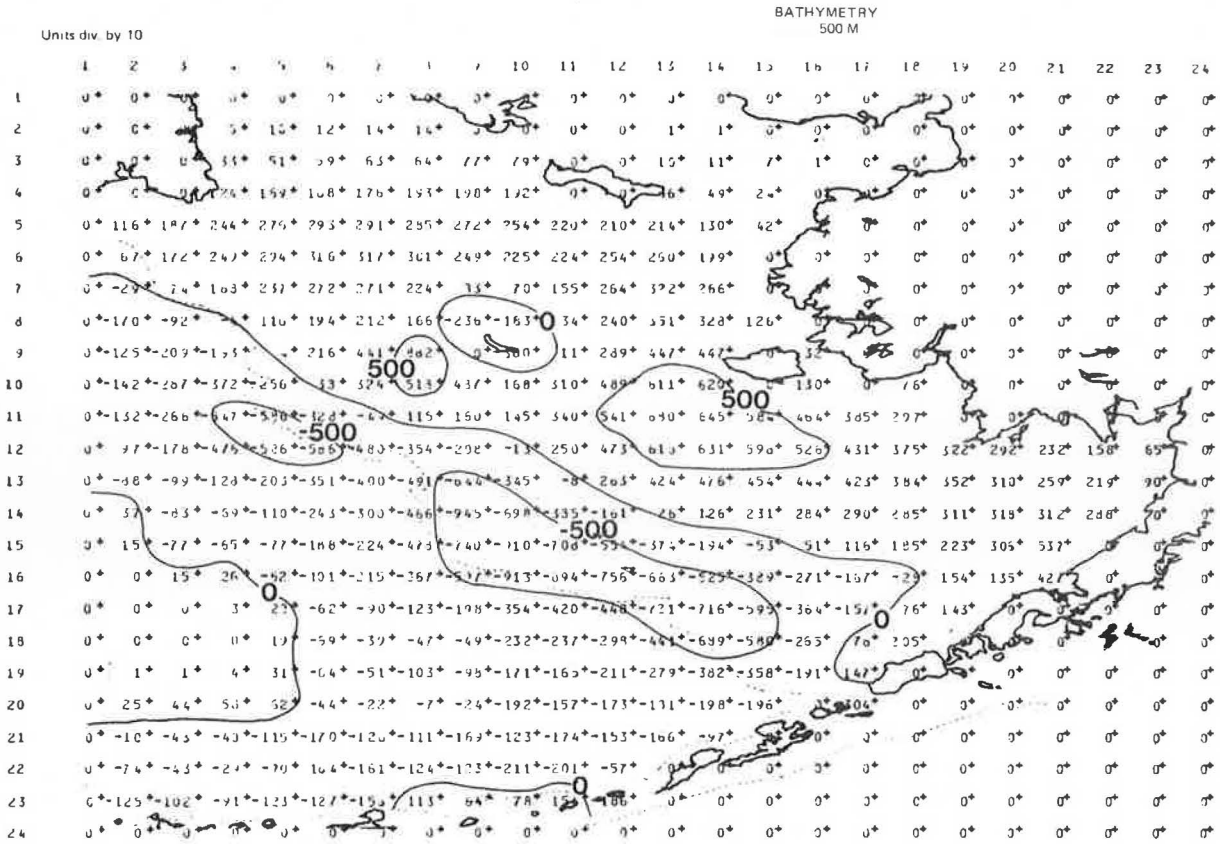


Figure 5c.--Monthly biomass change (in tens of kg/km²) of pollock due to seasonal migrations during April.

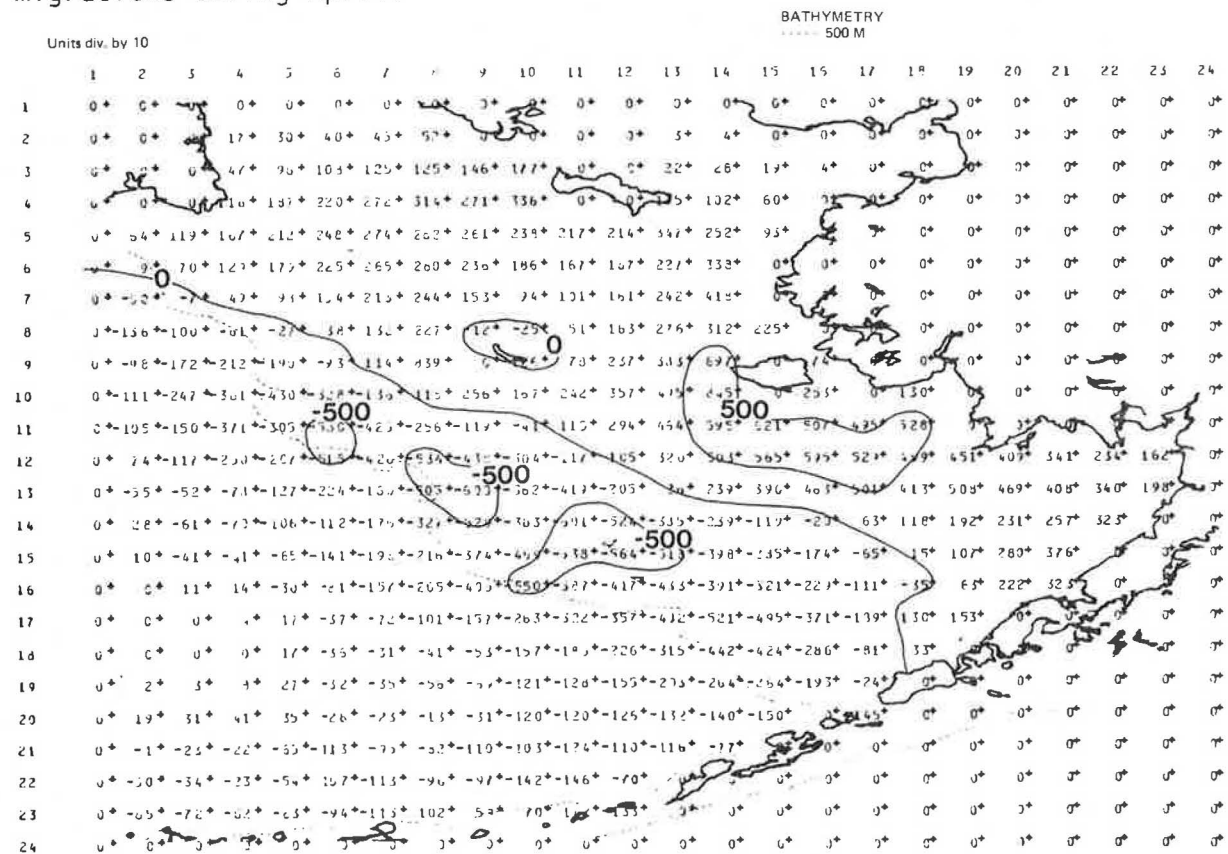


Figure 5d.--Monthly biomass change (in tens of kg/km²) of pollock due to seasonal migrations during May.

4. SIMULATION OF TEMPERATURE-INDUCED MIGRATIONS

The DYNUMES model simulates migrations to areas of optimum environment, using temperature as the main criterion. The computational procedures for the simulation of temperature-induced migration are similar to those used in the simulation of seasonal migrations; that is, the same three steps are followed. However, the initial estimate of velocity, the final velocity field, and the migrating fraction of the biomass are now all functions of temperature.

The model assigns an optimum temperature range for each species. Surface and bottom temperature fields for the Bering Sea for all twelve months have been compiled by Jim Ingraham of NWAFC, using over 50 years of data (Ingraham 1983) and are input to the model. The model compares the actual temperature at each grid point to the maximum and minimum optimum temperatures for each species to determine if migration will occur. Either the surface or bottom temperature field is used, depending on whether a particular species spends the majority of its life cycle nearer to the surface or to the bottom.

The temperature-induced migration velocity and migrating fraction of the biomass are calculated at each grid point. The DYNUMES model first checks the current month's temperature at a grid point against the minimum optimum temperature for the species. If the current month's temperature is less than the minimum, the velocity and the migrating fraction of the biomass are calculated as functions of: (1) the change in temperature from the previous month, (2) the difference between the current month's temperature and the species-specific minimum temperature, and (3) the latitude of the grid point. The model then checks the current month's temperature at the grid point against the maximum optimum temperature for the species and repeats the process. After

the fields of migrating fraction of the biomass and velocity have been calculated, the migrated biomass is computed in the manner previously described for seasonal migrations, using equation (1) with a time step of two days. Conservation of mass is then enforced by equation (5), the field is smoothed using equation (7), and, finally, the migrated biomass is added to the non-migrating biomass at each grid point.

The bottom temperature fields are used for both yellowfin sole and king crab. Mean bottom temperatures for May and June, shown in Fig. 7 (from Ingraham 1983), demonstrate the coastal warming occurring in bottom waters during spring months. The temperature-induced migration velocity vectors for May and June, shown in Fig. 8 (yellowfin and rock sole) and Fig. 9 (king crab), illustrate the shoreward migrations in response to this coastal warming. The surface temperature fields are used for pollock. Mean surface temperatures for May and June are shown in Fig. 10. At the surface, the warming trend is in a northward direction and isotherms are rather flat longitudinally until June. The temperature-induced migration velocity vectors for pollock during May and June, shown in Fig. 11, represent the northward migration response to the northward seasonal warming of Bering Sea surface water.

A comparison of the monthly biomass change due to seasonal migrations shown in Figs. 4, 5, and 6 with the monthly biomass change due to temperature-induced migrations during the same time periods demonstrates that seasonal migrations affect a much larger percentage of the biomass than do temperature-induced migrations, when using the mean monthly Bering Sea temperature data. However, at the present time, the DYNUMES model is being used to study the effects of anomalous environmental conditions (for example, extremes in ice cover, very warm or very cold years) on fish distributions.

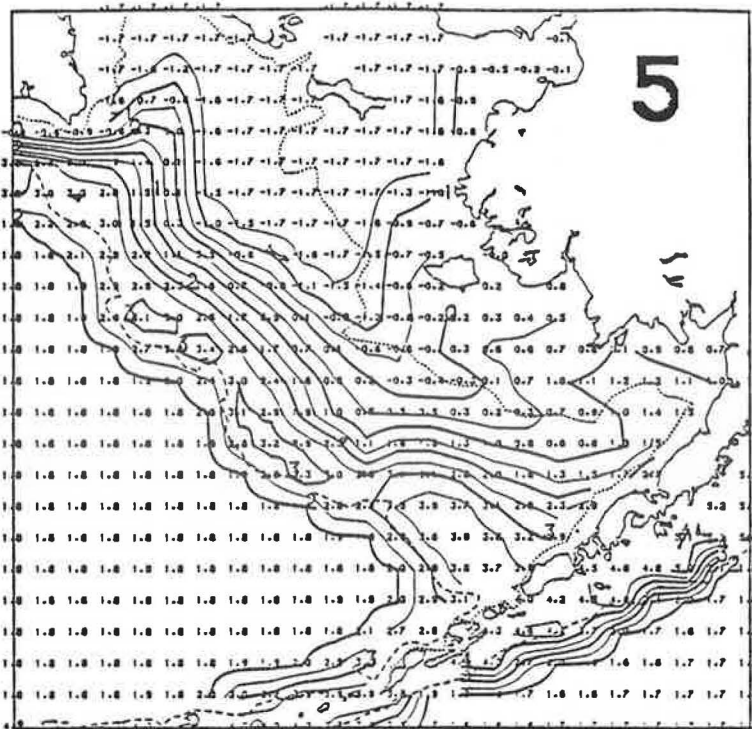


Figure 7b.--Mean Bering Sea bottom temperature for June (from Ingraham 1983).

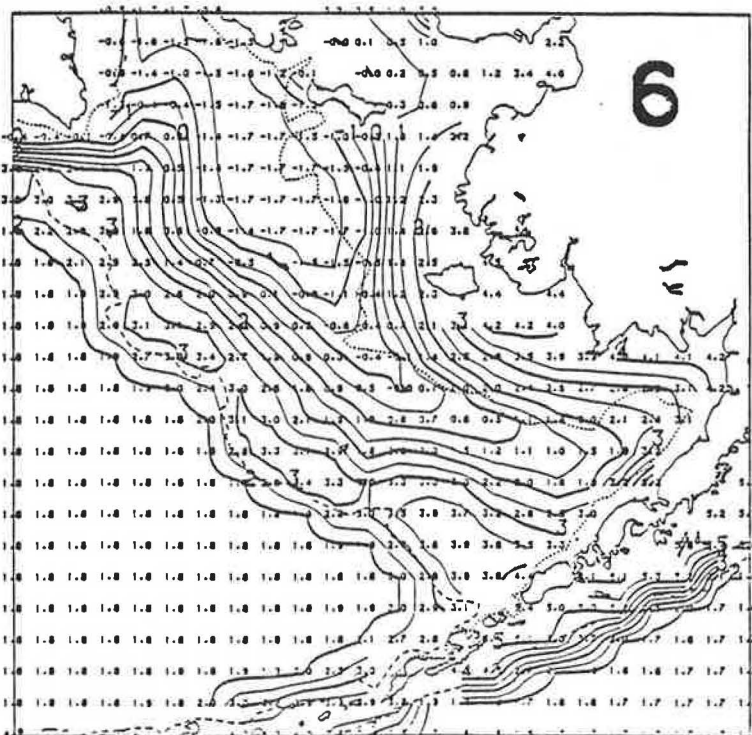


Figure 7a.--Mean Bering Sea bottom temperature for May (from Ingraham 1983).

VELOCITIES FOR TEMPERATURE-INDUCED MIGRATION
YEAR=2 MONTH=5 SPECIES=7

BATHYMETRY
50 M
500 M ----

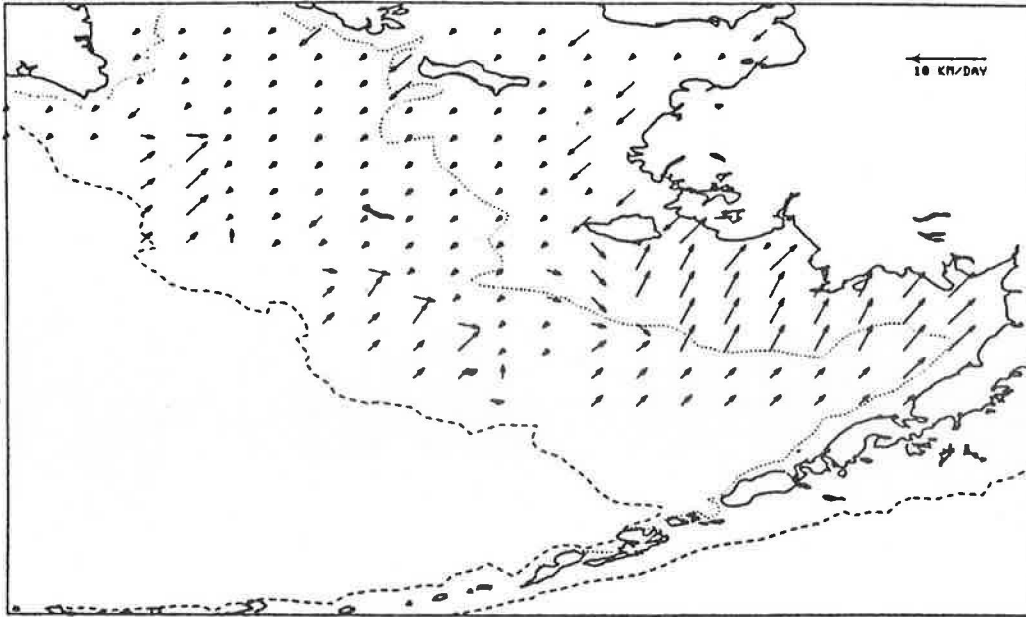


Figure 8a.--Velocity field (in km/day) for temperature-induced migrations of yellowfin and rock sole during May.

VELOCITIES FOR TEMPERATURE-INDUCED MIGRATION
YEAR=2 MONTH=6 SPECIES=7

BATHYMETRY
50 M
500 M ----

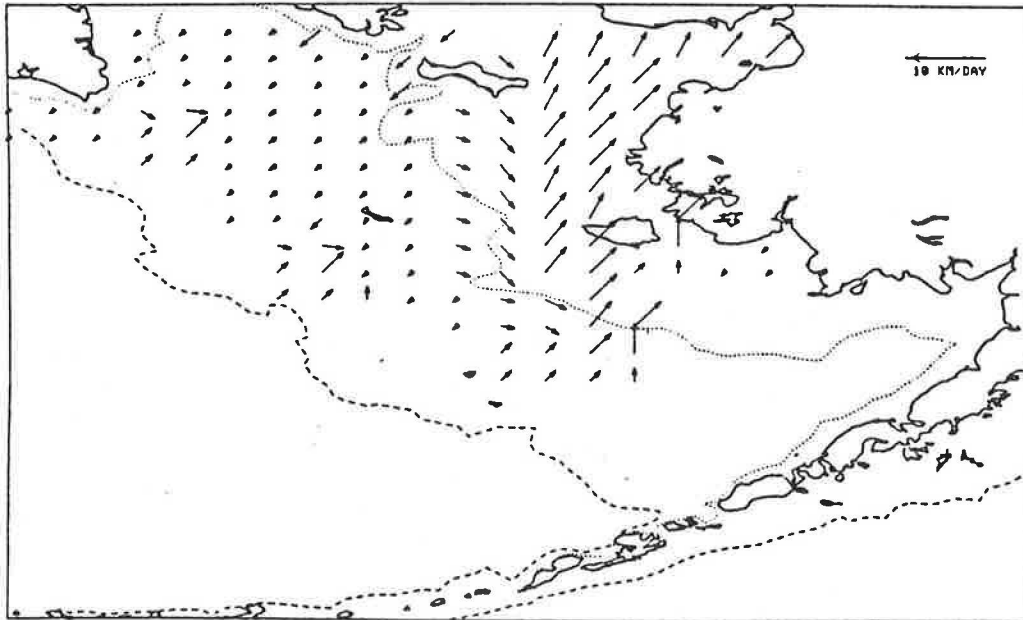


Figure 8b.--Velocity field (in km/day) for temperature-induced migrations of yellowfin and rock sole during June.

VELOCITIES FOR TEMPERATURE-INDUCED MIGRATION
YEAR=2 MONTH=5 SPECIES=19

BATHYMETRY
50 M
500 M - - - -

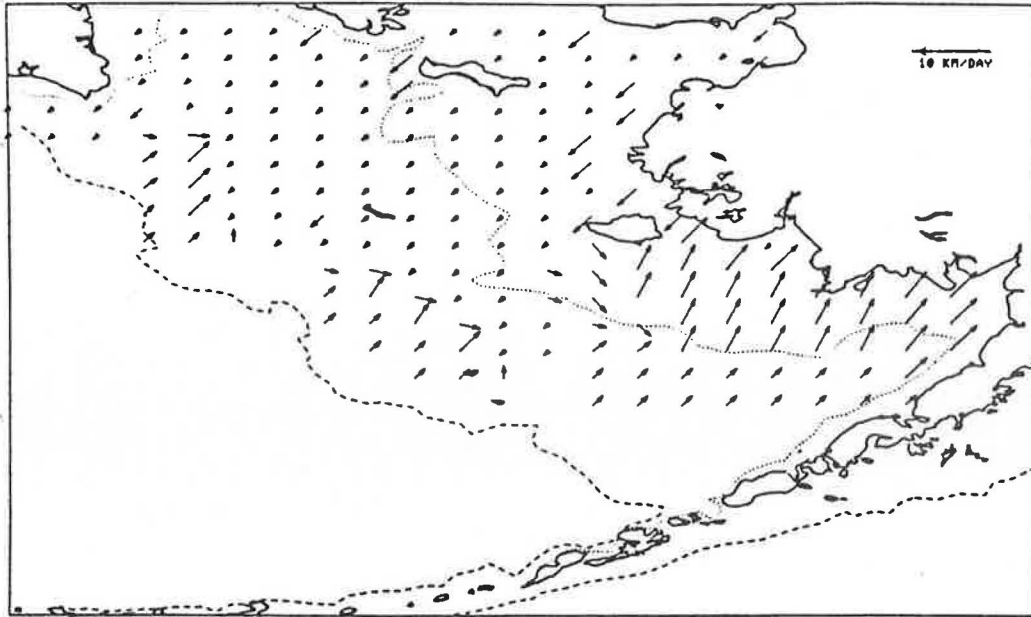


Figure 9a.--Velocity field (in km/day) for temperature-induced migrations of king crab during May.

VELOCITIES FOR TEMPERATURE-INDUCED MIGRATION
YEAR=2 MONTH=6 SPECIES=19

BATHYMETRY
50 M
500 M - - - -

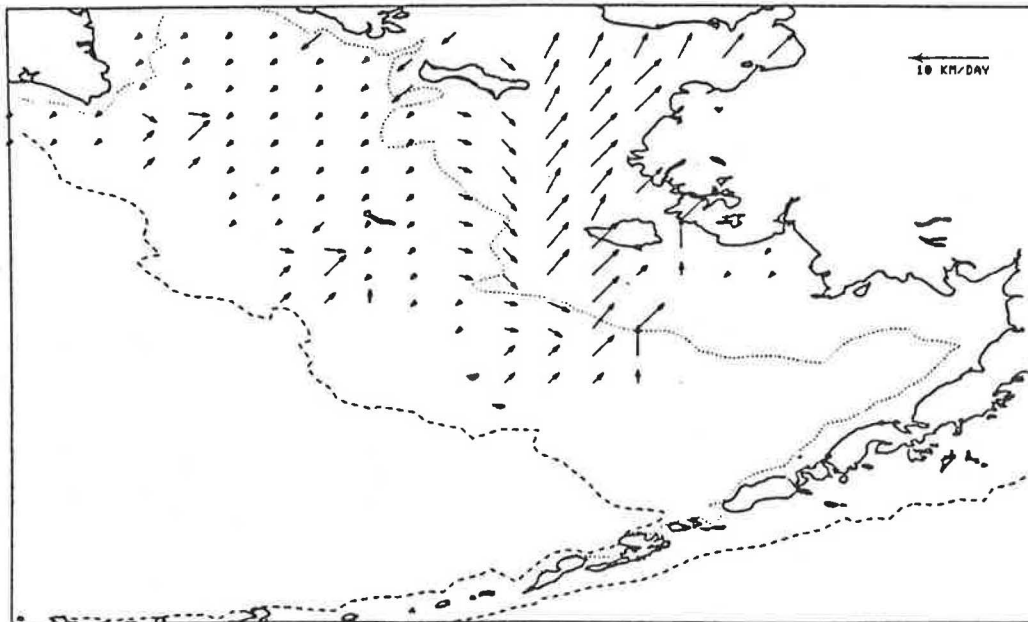


Figure 9b.--Velocity field (in km/day) for temperature-induced migrations of king crab during June.

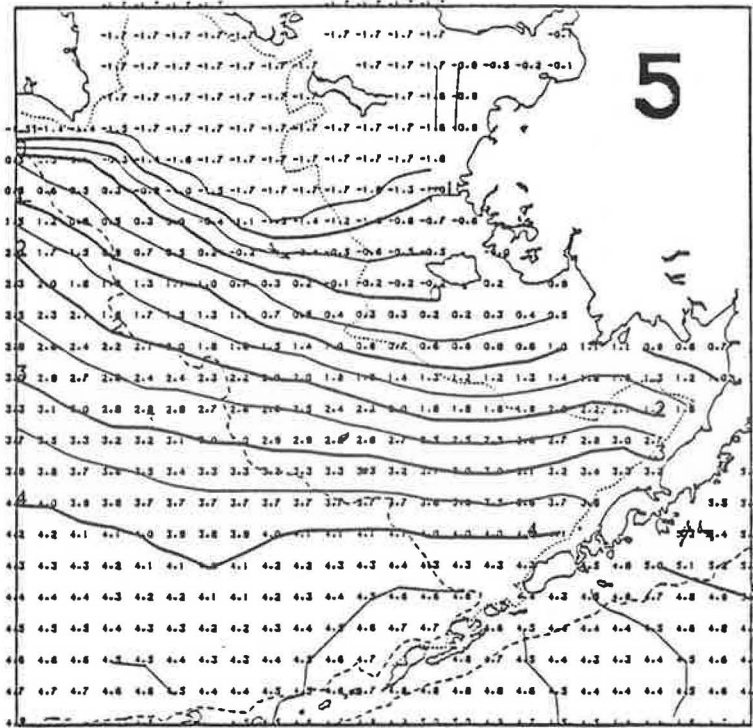


Figure 10a.--Mean Bering Sea surface temperature for May (from Ingraham 1983).

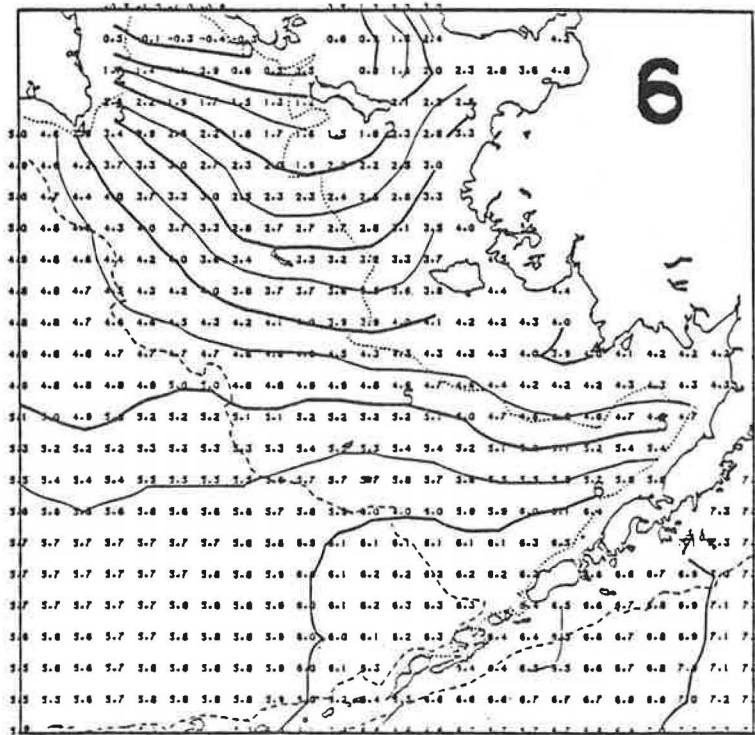


Figure 10b.--Mean Bering Sea surface temperature for June (from Ingraham 1983).

VELOCITIES FOR TEMPERATURE-INDUCED MIGRATION
YEAR=2 MONTH=5 SPECIES=12

BATHYMETRY
50 M
500 M -----

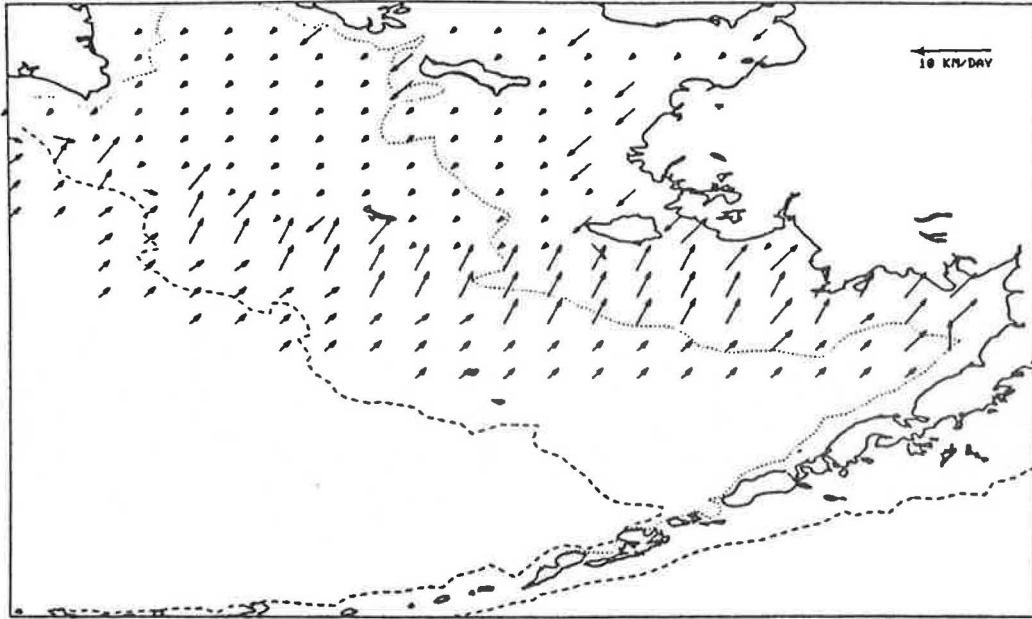


Figure 11a.--Velocity field (in km/day) for temperature-induced migrations of pollock during May.

VELOCITIES FOR TEMPERATURE-INDUCED MIGRATION
YEAR=2 MONTH=6 SPECIES=12

BATHYMETRY
50 M
500 M -----

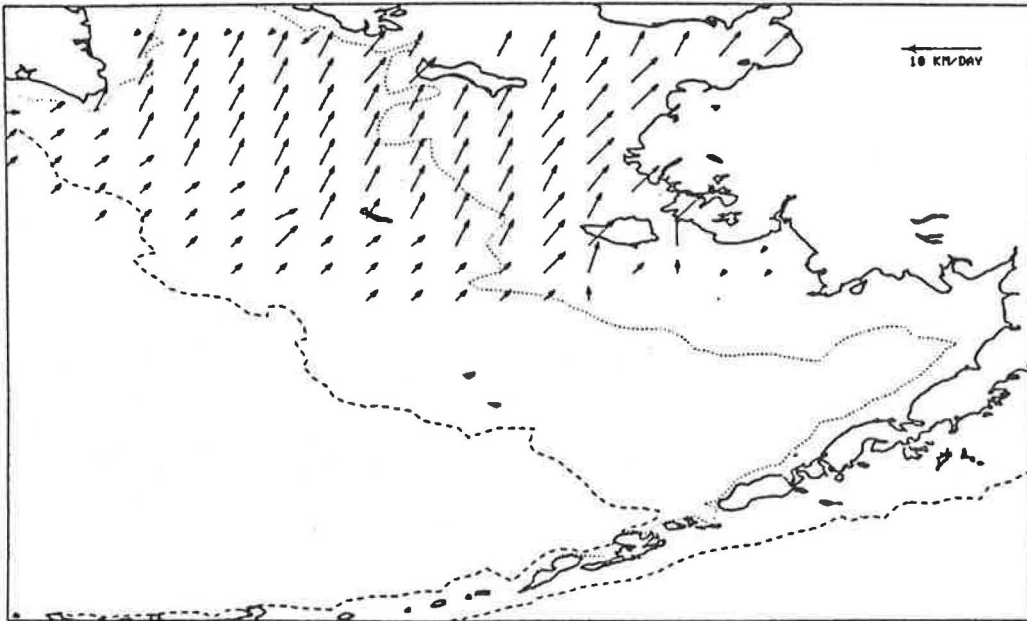


Figure 11b.--Velocity field (in km/day) for temperature-induced migrations of pollock during June.

5. RESULTS AND DISCUSSION OF MIGRATION SIMULATIONS

During each monthly time step of the DYNUMES model, the biomass at each Bering Sea grid point is adjusted for growth, predation mortality, and fishing mortality. The model is unique in its ability to simulate, in addition to these temporal changes, the spatial shifts in biomass observed in the Bering Sea. The effects of these spatial changes are illustrated by the summer (September) and winter (February) biomass distributions shown in Figs. 12 (yellowfin and rock sole), 13 (pollock), and 14 (king crab). Although the DYNUMES migration simulations redistribute the biomass with time in a gradual manner, it can be seen in Figs. 12, 13, and 14 that the locations of the maximum biomasses of migrating species undergo considerable seasonal shifts. On the other hand, the biomasses of non-migrating species groups such as infauna (species group 23) will fluctuate in time due to growth or predation, but the position of the maximum biomass distribution for sessile species groups will remain relatively constant over time. The DYNUMES model simulates predation using food composition tables for both shallow and deep water. Each food composition table consists of mean percentages of each prey species in each predator's diet. The percentages are modified by the model over time and space to reflect changes in food availability. The diet of migrating species such as yellowfin sole, which often preys upon sessile benthic organisms, must therefore undergo considerable change as it migrates to different areas in the Bering Sea. Only an ecosystem model such as DYNUMES, which simulates these temporal and spatial changes in predator-prey relationships occurring in the "real world", can be used to realistically describe this spatially variable ecosystem.

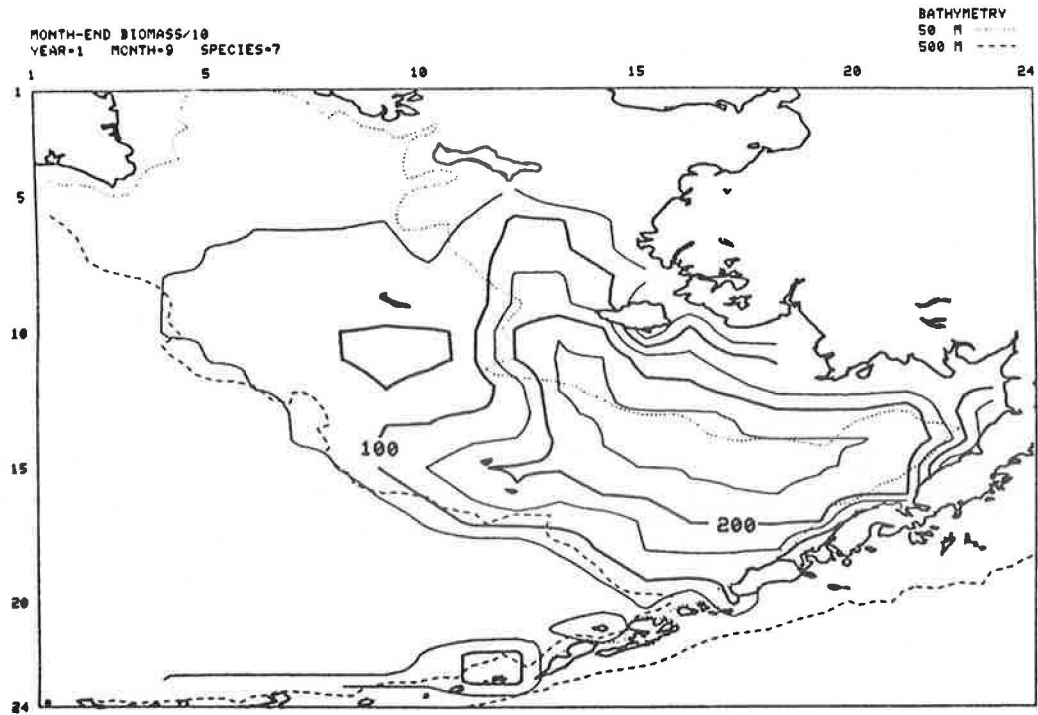


Figure 12a.--Summer (September) biomass distribution (in tens of kg/km^2) for yellowfin and rock sole.

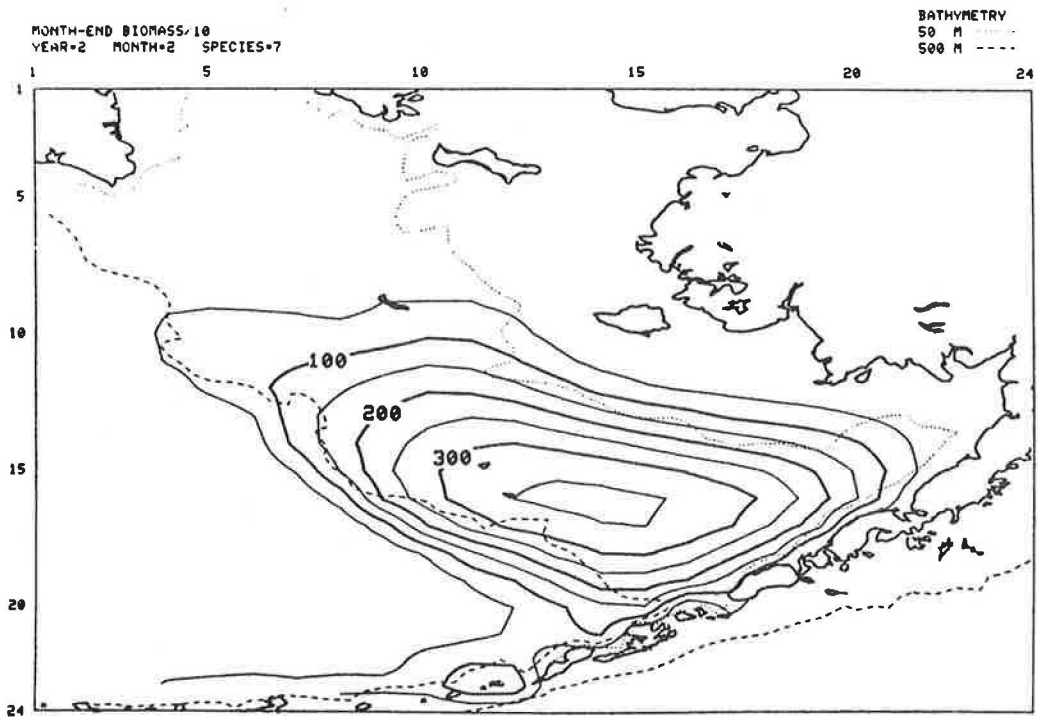


Figure 12b.--Winter (February) biomass distribution (in tens of kg/km^2) for yellowfin and rock sole.

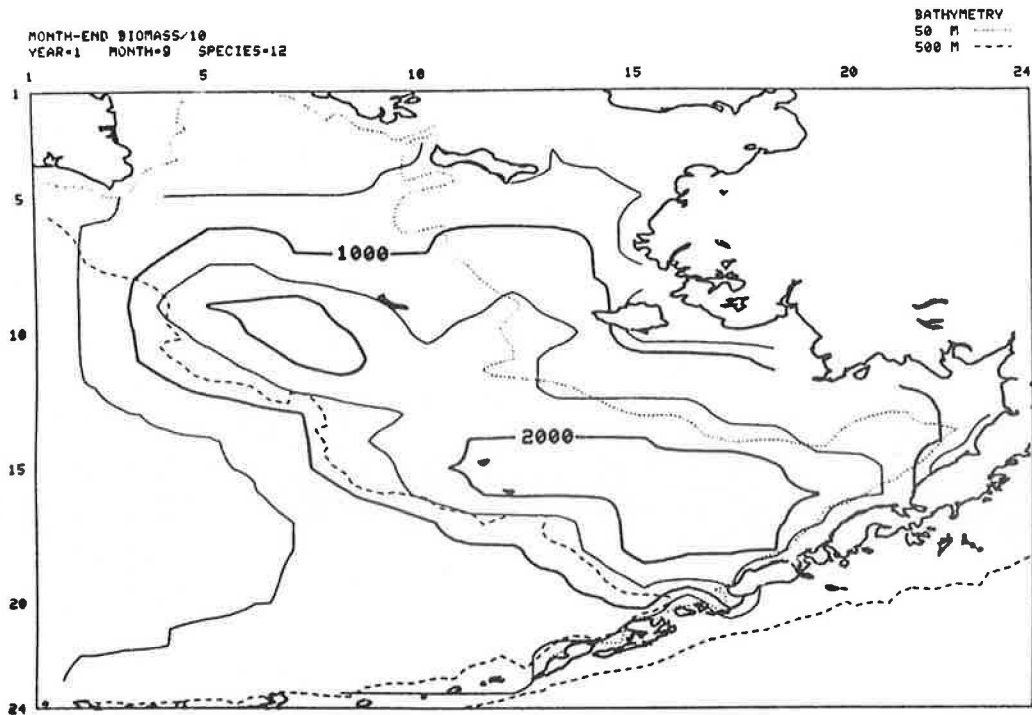


Figure 13a.--Summer (September) biomass distribution (in tens of kg/km²) for pollock.

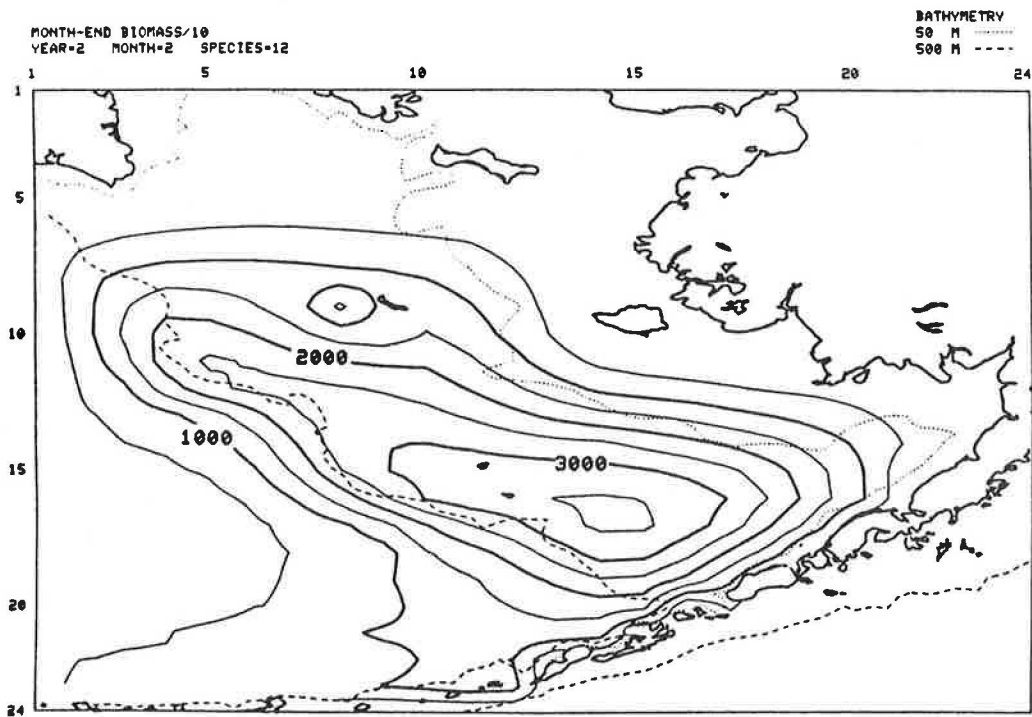


Figure 13b.--Winter (February) biomass distribution (in tens of kg/km²) for pollock.

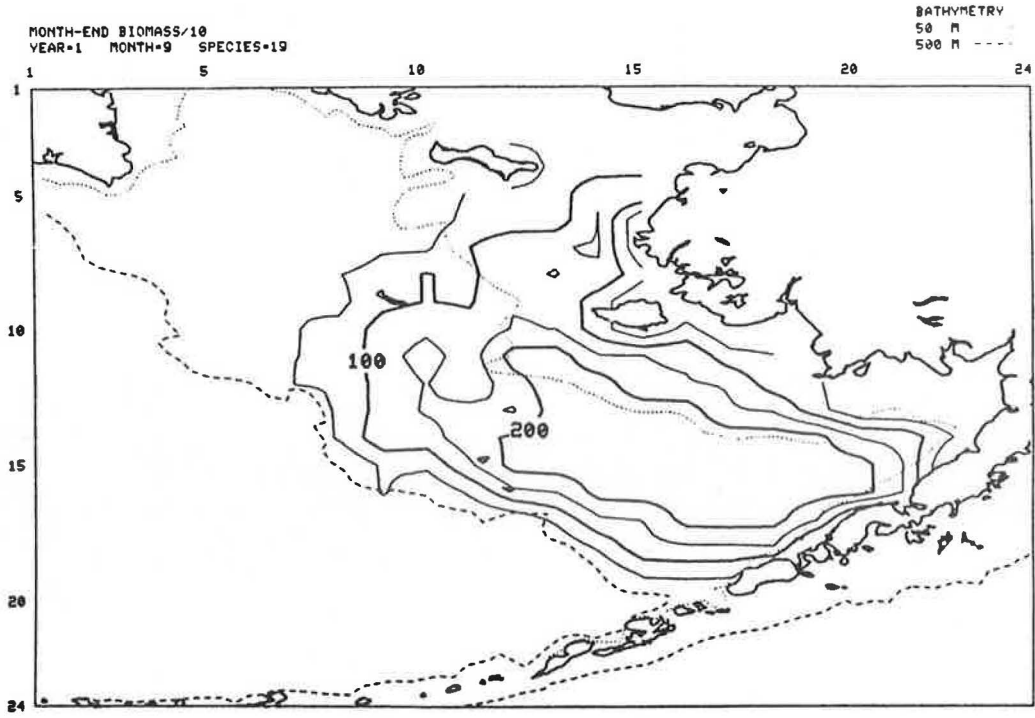


Figure 14a.--Summer (September) biomass distribution (in tens of kg/km^2) for king crab.

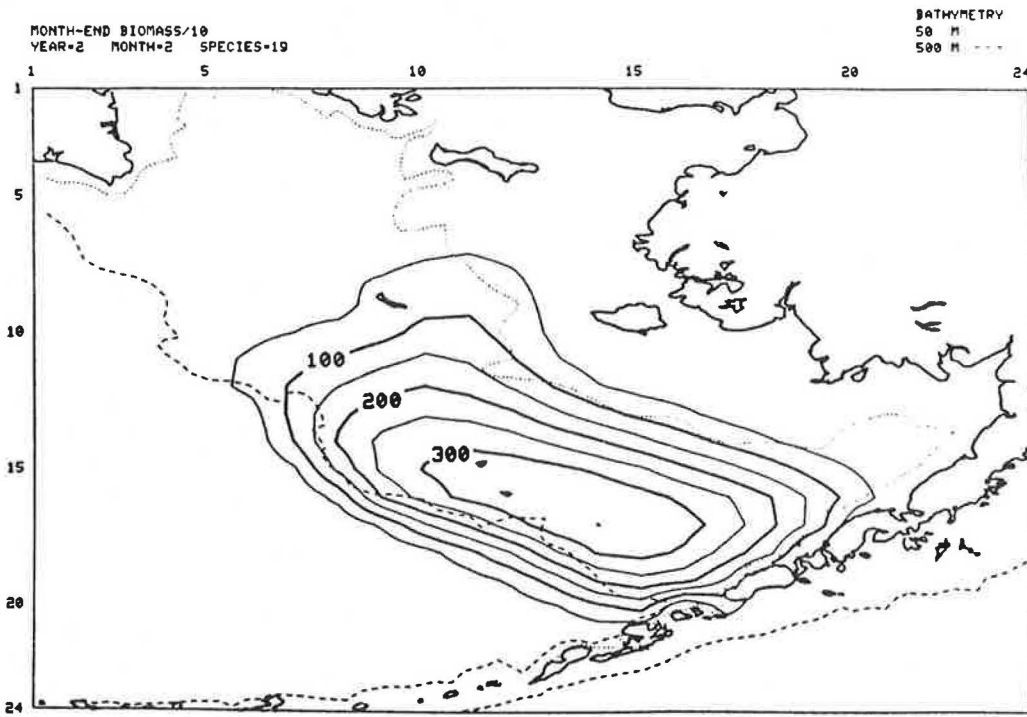


Figure 14b.--Winter (February) biomass distribution (in tens of kg/km^2) for king crab.

6. REFERENCES

Alverson, D.L.

1960. A study of annual and seasonal bathymetric catch patterns for commercially important groundfishes of the Pacific northwest coast of North America. Pacific Marine Fish. Comm. Bull. 4.

Bakkala, R.G.

1979. Population characteristics and ecology of yellowfin sole. In Fisheries oceanography - eastern Bering Sea shelf, Natl. Mar. Fish. Serv., Northwest and Alaska Fish. Cent., Seattle, WA, Processed Rep. 79-20, p. 280-329.

Bakkala, R.G. and G.B. Smith.

1978. Demersal fish resources of the eastern Bering Sea: Spring 1976. Natl. Mar. Fish. Serv., Northwest and Alaska Fish. Cent., Seattle, WA, Processed Rep., 233 pp.

Ingraham, J.W.

1983. A look at mean and anomolous temperature conditions in the eastern Bering Sea. Natl. Mar. Fish. Serv., Northwest and Alaska Fish. Cent., Seattle, WA, Processed Rep. (in preparation).

Laevastu, T.

1976. Predicting pollution dispersal with Hansen's hydrodynamical numerical models. In: (C. I. Bretschneider, ed.) Topics in ocean engineering, Vol. 3, Gulf Pub. Co., Houston, TX, p. 59-69.

Laevastu, T., J. Dunn, and F. Favorite.

1976. Consumption of copepods and euphausiids in the eastern Bering Sea as revealed by a numerical ecosystem model. Paper L:34, ICES C.M. 1976, Plankton Comm. 10 pp.

Laevastu, T., and F. Favorite.

1978. Numerical evaluation of marine ecosystem. Part II. Dynamical Numerical Marine Ecosystem Model (DYNUMES III) for evaluation of fisheries resources. Natl. Mar. Fish. Serv., Northwest and Alaska Fish. Cent., Seattle, WA, Processed Rep., 29 pp.

1979. Ecosystem dynamics in the eastern Bering Sea. In Fisheries oceanography - eastern Bering Sea shelf, Natl. Mar. Fish. Serv., Northwest and Alaska Fish. Cent., Seattle, WA, Processed Rep. 79-20, p. 444-481.

Laevastu, T. and R. Marasco.

1982. Evaluation of fishery resources with ecosystem simulations and quantitative determination of their response to ocean environmental anomalies and fishery. Natl. Mar. Fish. Serv., Northwest and Alaska Fish. Cent., Seattle, WA, Processed Rep. 82-08, 42 pp.

Niggol, K.

1982. Data on fish species from Bering Sea and Gulf of Alaska. U.S. Dep. Commer., NOAA Tech. Memo. NMFS F/NWC-29, 125 pp.

Pereyra, W.T., J.E. Reeves, and R.G. Bakkala.

1976. Demersal fish and shellfish resources of the eastern Bering Sea in the baseline year 1975. Natl. Mar. Fish. Serv., Northwest and Alaska Fish. Cent., Seattle, WA, Processed Rep., 619 pp.

Smith, G.B.

1979. The biology of walleye pollock. In Fisheries oceanography - eastern Bering Sea Shelf, Natl. Mar. Fish. Serv., Northwest and Alaska Fish. Cent., Seattle, WA, Processed Rep. 79-20, p. 213-279.

